AIP | Applied Physics Letters

Surface enhanced spin-flip scattering in lateral spin valves

Mikhail Erekhinsky, Amos Sharoni, Fèlix Casanova, and Ivan K. Schuller

Citation: Appl. Phys. Lett. **96**, 022513 (2010); doi: 10.1063/1.3291047
View online: http://dx.doi.org/10.1063/1.3291047
View Table of Contents: http://apl.aip.org/resource/1/APPLAB/v96/i2
Published by the American Institute of Physics.

Surface enhanced spin-flip scattering in lateral spin valves

Mikhail Erekhinsky,[1,a)] Amos Sharoni,[1] Fèlix Casanova,[1,2] and Ivan K. Schuller[1]
[1]*Department of Physics, University of California-San Diego, La Jolla, California 92093-0319, USA*
[2]*CIC nanoGUNE, 20018 Donostia-San Sebastian, and IKERBASQUE, Basque Foundation for Science, 48011 Bilbao, Basque Country, Spain*

(Received 2 July 2009; accepted 10 December 2009; published online 14 January 2010)

Nonlocal transport in Py/Cu lateral spin valves shows that the Cu spin diffusion length and the apparent Py spin polarization increase with Cu thickness. A proper quantitative analysis shows that the Cu spin diffusion length is dominated by surface spin-flip scattering and that the Py and Cu thickness dependence of spin polarization is due to strong spin-flip back-scattering at the Py/Cu interface. This solves a long-standing puzzle regarding the discrepancy in Py spin polarizations obtained from different measurements. Interestingly, the Cu surface oxidation causes enhanced spin diffusion, contrary to expectations. These surface effects substantially affect the performance of lateral spin valves. © *2010 American Institute of Physics*. [doi:10.1063/1.3291047]

The use of lateral spin valves in applications maybe hampered by the small magnitude of the spin valve signal.[1,2] As with the quest for increased signal in tunneling- or giant-magnetoresistance-based devices,[2,3] the signal enhancement in lateral devices is an ongoing challenge which may be the limit factor in eventual applications. These types of improvements can only be obtained by a serious effort geared to understand the role that device parameters and geometry play in this phenomenon.[3–5] Generally, in lateral spin valves there are two important controlling parameters: the polarization of injected current and the spin diffusion length. The polarization of injected current, depends on the intrinsic spin polarization of the ferromagnetic (FM) electrode[1,2] and the injection efficiency into the non-magnetic electrode (NM).[3,5–7] The spin diffusion length in the NM (Refs. 1–5) is the distance the injected spin imbalance diffuses before reaching its equilibrium value. Since metallic lateral spin valves are nanoscaled, surface effects may play a crucial role and maybe comparable to the bulk effects. Thus the surface may have a significant influence on both the spin injection efficiency and the spin diffusion length. In this letter we show that the performance of $Ni_{80}Fe_{20}$ permalloy/copper (Py/Cu) lateral spin valve with transparent interfaces is considerably enhanced with increasing Cu thickness and, contrary to naïve expectation, with increasing surface oxidation.

Performing non-local spin valve (NLSV) measurements[1] in samples with different Cu thicknesses and multiple devices we are able to separately determine the spin diffusion length in the Cu electrode (λ_{Cu}) and the effective spin polarization of Py (α_{Py}).[1] Both these parameters increase with increasing Cu thickness. The thickness dependence of λ_{Cu} and α_{Py} arise from different spin-flip scattering probabilities in the bulk Cu, at the Cu surface and at the Py/Cu interface.

The samples were fabricated by two-angle shadow evaporation,[8] which enables deposition of the Py and Cu electrodes on a Si substrate without breaking vacuum. This results in transparent and reproducible Py/Cu interfaces, which is crucial for these types of studies. Samples with six to eight lateral spin-valve devices in each sample were prepared under "identical" conditions, i.e., in the same pump down [Fig. 1(a)]. Each device consists of a pair of Py electrodes crossed by a common Cu strip. Edge-to-edge distance (d) between pairs of 35 nm thick Py electrodes was varied from 200 to 2000 nm. In every device, the width of one Py electrode (w_{Py}) is 100 nm and the other is 150 nm providing separate control over the magnetization of each electrode.[9] The Cu strip thickness (t_{Cu}) was varied between samples from 55 to 380 nm, and its width (w_{Cu}) was fixed at 250 nm for all samples.

Non-local measurements were performed using a conventional "dc reversal" technique[8] in a Helium-flow cryostat at 4.2 K. Details of the measuring scheme are described elsewhere.[8] The measured voltage depends on the relative orientation of magnetization of the two Py electrodes. It changes from a high value for parallel magnetization orientation to a low value for antiparallel [see Fig. 1(b)]. The difference between the high and low voltages normalized to the current magnitude, $\Delta V/|I|$, is denoted as the NLSV signal. The origin of the theoretically unpredicted asymmetry between high and low values was discussed in detail earlier.[8]

Figure 1(c) shows the typical NLSV signal (black squares) as a function of d for a sample with t_{Cu}=200 nm. The NLSV signal decreases with increasing distance between electrodes. This measurement combined with a theoretical description provides λ_{Cu} and α_{Py}, as described below.

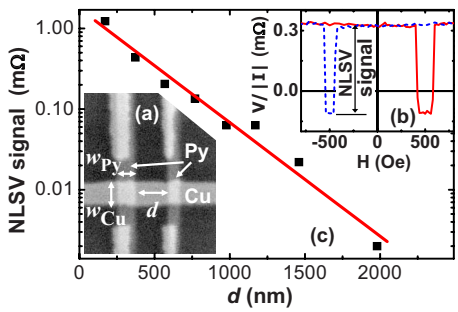

FIG. 1. (Color online) (a) Scanning electron micrograph of a typical device. Geometrical parameters are indicated in the image. (b) $V/|I|$ vs magnetic field for the device with d=370 nm. Solid red (dotted blue) line is for increasing (decreasing) field. The NLSV signal is marked. (c) NLSV signal (black squares) vs d for the sample with t_{Cu}=200 nm. Red solid curve is the fit to Eq. (1).

a)Electronic mail: merekhinsky@physics.ucsd.edu.

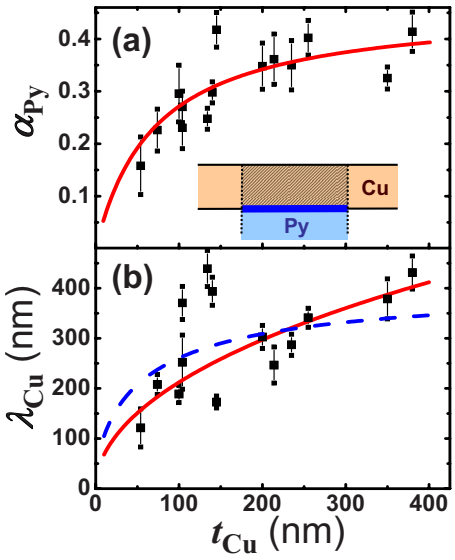

FIG. 2. (Color online) (a) α_{Py} (black squares) vs t_{Cu}. Red solid curve is a fit to the model for injected spins [Eq. (3)]. The inset is a schematic drawing showing a side view of the cross-shaped contact between the Cu strip (top) and the Py electrode (bottom). The shaded rectangle is the region of Cu strip right above the Py/Cu interface, which is marked by the thick line (blue online). (b) λ_{Cu} (black squares) vs t_{Cu}. Blue dashed line is a fitting curve for the modified spin diffusion model [Eq. (2)] accounting for all the Cu surfaces and red solid line assumes that only the top surface of Cu is relevant.

The one-dimensional spin-diffusion model with transparent interfaces applied to our geometry[9–11] provides an expression for the NLSV signal as a function of geometrical and material parameters

$$\frac{\Delta V}{|I|} = \frac{2\alpha_{Py}^2 R_{Cu}}{\left(2+\frac{R_{Cu}}{R_{Py}}\right)^2 \exp\left(\frac{d}{\lambda_{Cu}}\right) - \left(\frac{R_{Cu}}{R_{Py}}\right)^2 \exp\left(-\frac{d}{\lambda_{Cu}}\right)}, \quad (1)$$

where $R_{Cu}=2\lambda_{Cu}\rho_{Cu}/S_{Cu}$ and $R_{Py}=2\lambda_{Py}\rho_{Py}/S_{Py}(1-\alpha_{Py}^2)$ are spin-resistances, $\lambda_{Py,Cu}$ spin diffusion lengths, $\rho_{Py,Cu}$ resistivities, and $S_{Py,Cu}$ cross-sectional areas of Py and Cu. For all samples, we use $\lambda_{Py}=5$ nm (Refs. 1, 3, and 12) and $\rho_{Py}=19$ $\mu\Omega$ cm. ρ_{Py} was measured on a separate device deposited under nominally identical conditions, and is in agreement with values reported in the literature.[1,4,12] All other variables, ρ_{Cu}, S_{Py}, S_{Cu}, and d, were measured explicitly for each device. The data from each sample is fitted to Eq. (1) using α_{Py} and λ_{Cu} as fitting parameters. Figure 1(c) shows experimental data and the theoretical fit, which provide $\lambda_{Cu}=300\pm23$ nm and $\alpha_{Py}=0.35\pm0.04$. These values are in agreement with other NLSV measurements of the Py/Cu system,[1,4] although the effective spin polarization as usual is lower than that obtained by other methods.[3,13–16]

Figure 2(a) shows that α_{Py} (black squares) increases with Cu thickness and starts saturating above 200 nm. Figure 2(b) shows a tendency of increase (with some dispersion) of λ_{Cu} (black squares) as a function of t_{Cu}. We should note that each data point in this graph is obtained from a fitting for a different sample. Since each sample was deposited separately, the exact geometry and deposition conditions may vary from sample to sample giving origin to this dispersion. On the other hand, α_{Py} [Fig. 2(a)] has less dispersion, which implies that the Py/Cu interface is reproduced in different depositions.

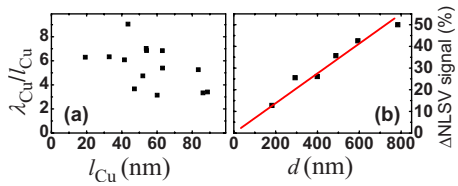

FIG. 3. (Color online) (a) λ_{Cu}/ℓ_{Cu} as a function of ℓ_{Cu}. (b) Increase of NLSV signal after oxidation (black squares) vs d for a sample with $t_{Cu}=210$ nm. Red solid line demonstrates a linear behavior of the NLSV signal increase vs d, indicating an increase in λ_{Cu} after oxidation.

The spin diffusion model predicts that to first approximation the decrease in electron spin polarization should be proportional to its diffusion time inside the NM.[3,9] Therefore, the spin diffusion length should be proportional only to the electron mean free path in the Cu strip (ℓ_{Cu}),[5] implying that the ratio λ_{Cu}/ℓ_{Cu} should be constant. Figure 3(a) shows λ_{Cu}/ℓ_{Cu} as a function of ℓ_{Cu}, which was determined independently from the resistivity of Cu measured for each sample.[17] The large fluctuations of λ_{Cu}/ℓ_{Cu} with ℓ_{Cu} imply the presence of an additional spin-flip mechanism besides the scattering which limits the mean free path. An obvious location for this additional spin-flip scattering is at the Cu surface, implying that the spin diffusion length in Cu will change with thickness. For this reason, we include surface effects into the derivation of the one-dimensional diffusion equation.[18] To account for the bulk spin-flip scattering we assume each momentum scattering has a probability p_b to also flip the spin. We included different probability p_s to characterize the surface spin-flip. With this, the dependence of λ_{Cu} on the Cu strip geometry is

$$\lambda_{Cu} = \frac{\ell_{Cu}}{\sqrt{6p_b + \ell_{Cu}p_s\left(\frac{2}{t_{Cu}}+\frac{2}{w_{Cu}}\right)}}. \quad (2)$$

A fit to Eq. (2) [blue dashed curve in Fig. 2(b)], which follows the general trend of λ_{Cu} versus t_{Cu}, gives $p_b=1.0\times10^{-4}\pm1.4\times10^{-3}$ and $p_s=0.036\pm0.024$. However, an improved fit [red solid curve in Fig. 2(b)] is obtained if the spin-flip scattering from the side surfaces is excluded. This indicates that the main surface spin flip arises from the top surface or the Cu/Si substrate interface. In this case, the corresponding probabilities are $p_b=1.0\times10^{-4}\pm7.4\times10^{-4}$ and $p_s=0.14\pm0.06$. In either case, the surface spin-flip scattering probability is three orders of magnitude larger than the bulk. This leads to the interesting conclusion that the spin diffusion length of Cu is dominated by surface scattering. With increasing Cu thickness, the bulk contribution to spin-flip scattering becomes more important. The relative importance of the surface to bulk contribution depends on w_{Cu}, t_{Cu}, and ρ_{Cu}, varies with deposition method and geometry of the device. Since all these are different from experiment to experiment, the low temperature values of λ_{Cu} found by us and reported in the literature are in the range of 120–1000 nm.[1,3,4,8,12,19] Enhanced spin-flip scattering from metal surfaces was suggested earlier although not quantified by others[12,20,21] and also found in recent theoretical calculations.[22]

Additional interesting and unexpected results were obtained by oxidizing a few samples and re-measuring the NLSV signal. Figure 3(b) shows the percentage difference

between NLSV signals in the 210 nm sample before and after oxidation. The NLSV signal increases substantially for each device, giving rise to an increase of λ_{Cu} from 247 ± 36 nm to 282 ± 48 nm. Since the Cu/Si interface is probably not affected by the oxidation, the increase in λ_{Cu} implies that it is the top surface which provides strong spin-flip scattering. We note that α_{Py} does not change with oxidation, indicating that, as expected, the Py/Cu interface properties are not affected.

Again the dependence of α_{Py} on t_{Cu} cannot be explained by the one-dimensional spin-diffusion model because in this model the spin polarization is an intrinsic parameter of the FM. The one-dimensional model does not consider the region of the Cu strip above the Py/Cu interface [see inset of Fig. 2(a)]. This region is an intermediate stage for electrons after they have been injected into Cu and before diffusing further along the Cu strip. Injected electrons carry into the Cu the intrinsic polarization of Py due to negligible spin-flip scattering at the interface.[3] However, during diffusion in this "intermediate" Cu region, scattering of electrons occurs in the Cu bulk, and at the Cu surfaces, providing spin-flip scattering. Moreover, electrons maybe back-scattered to the Py/Cu interface, enhancing spin flipping due to the magnetic nature of the interface. Therefore, the injected electrons will experience considerable spin polarization loss even before diffusion along the Cu strip. As a consequence, the fitted parameter α_{Py} is an *effective* spin polarization of Py and is smaller than the intrinsic polarization.

To calculate the effective polarization of the injected electrons, spin-flip scattering from the bulk of Cu, the Cu surface and the Cu/Py interface must be included. With N_{In} the number of injected polarized electrons per unit time, and N_{Out} the number leaving the area above the injector, $\alpha_{Py} = \alpha_{int}(N_{Out}/N_{In})$ where α_{int} is the intrinsic polarization of Py. $N_{Out}=N_{In}-N_{Scatt}$ where N_{Scatt} is the number of spins per unit time which scatter in the region above the Py electrode. These include spins scattered at the Cu surface, in the Cu bulk and at the Py/Cu interface, and are functions of the scattering probabilities p_s, p_b, and p_i (the spin-flip probability for momentum scattering at the Py/Cu interface), the geometrical parameters (t_{Cu}, w_{Cu}, w_{Py}) and ℓ_{Cu}. Solving for the steady state:

$$\alpha_{Py} = \frac{\alpha_{int}}{1 + p_b \frac{3w_{Py}}{\ell_{Cu}} + \frac{w_{Py}}{2}\left(\frac{p_s + p_i}{t_{Cu}} + \frac{2p_s}{w_{Cu}}\right)}. \quad (3)$$

An excellent fit [red solid curve in Fig. 2(a)] is obtained using this formulation, with p_s and p_b obtained previously, and w_{Py} measured separately for each device. The adjustable parameters obtained this way are $p_i = 1.0 \pm 0.4$ and $\alpha_{int} = 0.50 \pm 0.07$. The fit quality and parameters are independent of the inclusion of all free Cu surfaces or only the top surface. The value $p_i = 1$ is reasonable, implying that each back-scattered electron that reaches the magnetic Py/Cu interface completely loses spin information. This is equivalent to spin absorption due to the introduction of an additional spin relaxation channel.[4] More importantly, this also solves a long standing puzzle by recovering a value $\alpha_{int} = 0.50$ in agreement with values obtained by other methods (0.35–0.8).[13–16]

To summarize, we investigated the dependence of the spin diffusion length of Cu and the effective spin polarization of Py on Cu thickness using Py/Cu lateral spin valves with transparent contacts. Quantitative analysis reveals strong spin-flip scattering at the surface of Cu. This surface scattering is dominant for thinner Cu strips and considerably reduces the spin diffusion length of Cu. Interestingly, oxidation of the Cu strip reduces the surface spin-flip scattering. In addition, the effective spin polarization injected from Py is strongly affected by the presence of the Py/Cu interface in thinner Cu strips. Moreover, including surface effects and back-scattering into the FM electrodes into the analysis of spin diffusion in lateral spin valves reconciles the long standing apparent contradiction regarding values of injected spin polarization obtained from different measurements. The limitations in spin injection and transport due to surface scattering and interface back-scattering in lateral nanostructured devices may be overcome by proper surface manipulation (such as oxidation) and the use of smaller junction areas.[4] This also shows that an increased understanding of the origin of enhanced spin-flip scattering at the surfaces,[22] is crucial for the development of future multiterminal spintronic devices.

We thank Professor J. Bass, Professor W.P. Pratt, and Professor N. Birge for interesting correspondence and Professor H. Suhl for illuminating discussions. This work was funded by the U.S. DOE.

[1] F. J. Jedema, A. T. Filip, and B. J. van Wees, Nature (London) **410**, 345 (2001).
[2] I. Žutić, J. Fabian, and S. D. Sarma, Rev. Mod. Phys. **76**, 323 (2004).
[3] J. Bass and W. P. Pratt, J. Phys.: Condens. Matter **19**, 183201 (2007).
[4] T. Kimura and Y. Otani, J. Phys.: Condens. Matter **19**, 165216 (2007).
[5] N. Poli, M. Urech, V. Korenivski, and D. B. Haviland, J. Appl. Phys. **99**, 08H701 (2006).
[6] S. O. Valenzuela and M. Tinkham, Appl. Phys. Lett. **85**, 5914 (2004).
[7] A. Fert and S.-F. Lee, Phys. Rev. B **53**, 6554 (1996).
[8] F. Casanova, A. Sharoni, M. Erekhinsky, and I. K. Schuller, Phys. Rev. B **79**, 184415 (2009).
[9] F. J. Jedema, M. S. Nijboer, A. T. Filip, and B. J. van Wees, Phys. Rev. B **67**, 085319 (2003).
[10] T. Kimura, J. Hamrle, and Y. Otani, Phys. Rev. B **72**, 014461 (2005).
[11] T. Valet and A. Fert, Phys. Rev. B **48**, 7099 (1993).
[12] T. Kimura, T. Sato, and Y. Otani, Phys. Rev. Lett. **100**, 066602 (2008).
[13] S. Dubois, L. Piraux, J. M. George, K. Ounadjela, J. L. Duvail, and A. Fert, Phys. Rev. B **60**, 477 (1999).
[14] P. Holody, W. C. Chiang, R. Loloee, J. Bass, W. P. Pratt, and P. A. Schroeder, Phys. Rev. B **58**, 12230 (1998).
[15] B. Nadgorny, R. J. Soulen, M. S. Osofsky, I. I. Mazin, G. Laprade, R. J. M. van de Veerdonk, A. A. Smits, S. F. Cheng, E. F. Skelton, and S. B. Qadri, Phys. Rev. B **61**, R3788 (2000).
[16] R. J. Soulen, Jr., J. M. Byers, M. S. Osofsky, B. Nadgorny, T. Ambrose, S. F. Cheng, P. R. Broussard, C. T. Tanaka, J. Nowak, J. S. Moodera, A. Barry, and J. M. D. Coey, Science **282**, 85 (1998).
[17] A. Abrikosov, *Fundamentals of the Theory of Metals* (Elsevier, Amsterdam, 1988).
[18] M. E. Glicksman, *Diffusion in Solids* (Wiley, New York, 2000).
[19] Y. Ji, A. Hoffmann, J. E. Pearson, and S. D. Bader, Appl. Phys. Lett. **88**, 052509 (2006).
[20] J. Vranken, C. Van Haesendonck, and Y. Bruynseraede, Phys. Rev. B **37**, 8502 (1988).
[21] F. Pierre and N. O. Birge, Phys. Rev. Lett. **89**, 206804 (2002).
[22] H. Suhl (unpublished).